

INSTRUMENTS AND METHODS OF INVESTIGATION PACS numbers: 89.60.Gg, 91.30.Nw, 92.05.Bc, 92.05.Hj, 92.10.hl, 92.10.Hm

Tsunami wave suppression using submarine barriers

A M Fridman, L S Alperovich, L Shemer, L Pustil'nik,
D Shtivelman, An G Marchuk, D Liberzon

DOI: 10.3367/UFNe.0180.201008d.0843

Contents

Abstract. **Submerged barriers, single or double, can be used to greatly reduce the devastating effect of a tsunami wave according to a research flume study conducted at Tel Aviv University.**

1. Introduction

Tsunami, Japanese for "a big harbor wave," is one of the most dangerous natural calamities affecting the coastal zone of world's oceans. They occur most frequently in the Pacific because seismic activity there is much higher than in other oceans. Indeed, in an overwhelming number of cases, tsunamis are generated by strong underwater earthquakes. Eruptions of submarine volcanos, submarine landslides, and the impact of large meteorites are among other factors having the potential to generate tsunamis.

In addition to the Pacific, tsunamis are also observed in the Atlantic and Indian Oceans. There are data on tsunamis in the Mediterranean Sea [1] and even in the Black and Caspian Seas [2]. The damage caused by strong tsunamis sometimes far exceeds that from the tsunamigenic earthquake proper. The most common tsunami generation mechanism is an abrupt vertical displacement of large areas in the epicentral region (or its vicinity) accompanying strong submarine earthquakes. It cannot be excluded that tsunamis are generated by massive submarine landslides and the fall of large soil masses from steep slopes.

On average, about three thousand submarine earthquakes occur each year on Earth [3]. A fraction of the seismic source energy is transformed into that of wave motion. Accordingly, strong submarine earthquakes might provoke disastrous tsunamis [4]: in 2004 alone, the death toll was more than 230 000 in over 11 countries across the Asia–Pacific region as the result of a massive tsunami in the Indian Ocean.

One of the intrinsic characteristics of tsunamis is their ability to propagate over huge distances while preserving the devastating power. During the Chilean tsunami, the waves traversed the entire Pacific Ocean in 22 hours and hit the Japanese coast, causing considerable damage. The tsunami propagation speed in the open ocean is reliably predicted by the formula $c = \sqrt{gH}$, where H is the water depth and g the acceleration of gravity. This formula assumes the ocean to be shallow compared to the tsunami wavelength. The mean depth of the Pacific Ocean is about 4 km, and the tsunami propagation speed there is about 700 km h^{-1}. Detecting tsunamis in the open ocean is practically impossible without dedicated instruments because their wavelength lies in the range from several dozen to several hundred kilometers, while their amplitude is only 1–2 m. The initial sea surface elevation in the tsunami source region does not exceed a few meters, while the wave periods are in the range from 2 to 200 min. The wave amplitude is reduced with distance from the source due to cylindrical divergence, except the cases where the tsunami propagates along submarine ridges that serve as waveguides. In the latter case, the amplitude stays practically constant.

Because of a relatively weak damping with distance from the source and the wave energy focusing due to the varying bottom topography and Earth's sphericity, even the tsunamis excited by fairly distant sources are dangerous. Wave refraction over uneven bottom topography modifies the direction of wave front propagation and may result in an extremely irregular wave amplitude distribution along the coastline.

A M Fridman Institute of Astronomy, Russian Academy of Sciences,
ul. Pyatnitskaya 48, 119017 Moscow, Russian Federation
Russian Research Center "Kurchatov Institute",
pl. Akademika Kurchatova 1, 123182 Moscow, Russian Federation
Department of Geophysics and Planetary Sciences,
Tel Aviv University, Israel
Tel. (7-495) 951-79 93. E-mail: fxela11@yahoo.com.
L S Alperovich, L Pustil'nik, D Shtivelman Department of Geophysics and Planetary Sciences, Tel-Aviv University, Israel
E-mail: lalperovich@gmail.com, levpust@post.tau.ac.il
L Shemer, D Liberzon School of Mechanical Engineering,
Tel-Aviv University, Israel
E-mail: shemer@eng.tau.ac.il
An G Marchuk Institute of Computational Mathematics
and Mathematical Geophysics SB RAS
prosp. Akademika Lavrent'eva 6, 630090 Novosibirsk,
Russian Federation
E-mail: mikh@sscc.ru

Received 29 December 2009, revised 2 April 2010
Uspekhi Fizicheskikh Nauk **180** (8) 843 – 850 (2010)
DOI: 10.3367/UFNr.0180.201008d.0843
Translated by S D Danilov; edited by A M Semikhatov

Figure 1. Wave-breaking barrier in the mouth of Ofunato Bay in northeast Japan built for tsunami protection.

When tsunamis enter the shallow ocean, their propagation speed decreases drastically. The amplitude grows accordingly and reaches a maximum value along the zero depth line (if the wave crest does not break). The lateral confinement of a tsunami, e.g., entering a narrow bay or river mouth entails even stronger growth in the wave amplitude.

Theoretical approaches to the problem of tsunami generation, propagation, transformation, and dissipation were the subject of studies [5, 6] and [7]. Theoretical predictions are typically supported by numerical simulations. Book [8] offers a thorough review of the main results of more than 50 authors worldwide pertaining to numerical modeling of nonlinear waves in the ocean, such as waves generated by landslides, solitary waves, or tsunamis, their interaction with coastal areas, and so on. The numerical models developed in [9–11] laid the basis for the tsunami zoning of the Russian Pacific coast, including estimates of the tsunami occurrence probability in a given region and the vulnerability to flooding as a function of the tsunami parameters.

While the importance of numerical simulation of tsunami generation and propagation is beyond all doubts, it is also quite apparent that some effects can be lost even in simulations performed for the simplest models of bottom topography, such as underwater ridges, which frequently channel the waves or hinder their propagation. This can distort even a qualitative picture of the phenomenon.

Such difficulties occur because a tsunami propagating over such a bottom excites wave perturbations over a range of scales from a few hundred kilometers down to that of local turbulence. For a wave propagating along an underwater ridge or reef, waveguide trapping is possible. A new scale — the transverse obstacle size — emerges in this case. In contrast, if the wave impinges on this two-dimensional obstacle transversely, small-scale perturbations may evolve, breaking up downstream of the submarine obstacle. Such perturbations may introduce additional dissipation to the original large-scale wave through the accompanying 'turbulent' viscosity. In contrast, submerged islands may focus a tsunami locally such that it experiences substantial growth in the lee of an island and, consequently, noticeable attenuation some distance away [12].

Because the momentum flux density tensor is proportional to the velocity squared [13], it is natural to try to reduce the wave impact strength and the resulting damage by reducing the fluid velocity, for example, by placing an obstacle across the fluid path. Results of laboratory modeling in the early 1960s showed that an obstacle crossing the path of a strong tsunami reduces not only the depth of runup but also the velocity of the onshore watermass flow. One engineering solution to shelter population and infrastructure from tsunamis is the construction of protective walls of various kinds separating harbors from the main territory of settlements and towns. The height of such walls reaches 5 m. Figure 1 presents a photograph of a protective pier in Ofunato Bay (Japan) (the total pier length is 740 m, leaving a 200 m wide entrance to the bay), capable of withstanding tsunamis up to 6 m in height (unsubmerged barriers). Built in 1967, the barriers proved their efficiency just one year later during the tsunami on 16 May 1968, reducing the tsunami height twofold.

Such barriers are in principle capable of protecting harbor constructions against a tsunami of moderate strength, but for a strong event, even solid concrete walls rising over water yield to the tsunami water head and topple over. During the strong tsunami in 1983, water flowed over walls 6 m in height in the Nosiro harbor, and several blocks weighting 5000 t each were overturned.

Consequently, from this standpoint, it is advisable to use one or several submerged barriers that do not fully suppress tsunamis but substantially mitigate their hazard to seacoast communities. Indirect evidence in favor of such an approach is provided by the recently published data on a substantial mitigation of destructive tsunami consequences in zones on the shore that are protected by coral reefs. Conversely, in locations where the reefs were damaged or destroyed through illegal trade, the damage caused by tsunamis was particularly devastating. Based on multiple data sources, the International Maritime Organization [14] (2009) pointed to the important role of submarine coral reefs in protecting against tsunami disasters.

Theoretical and numerical models of the response from a vertical unsubmerged barrier to the propagation of a traveling tsunami wave have been under study since the 1960s (see Refs [15–22]).

2. Experimental study of the effect of submerged barriers on wave propagation

We have experimentally explored the impact of single and double submerged barriers on the propagation of a solitary wave package with the characteristic horizontal scale exceeding the water layer depth by a factor of 10–30. Here, we discuss the results of our experiments pertaining to simulation of tsunamis and their mitigation. The experiments were performed in one of the specialized basins located in the building of the Engineering Department of Tel-Aviv University. The Department runs two experimental channels,

Figure 2. Two experimental channels used for laboratory simulations of small and large-scale wave and hydrodynamic phenomena. The length of the left channel is 20 m (a) and the length of the right one, used for tsunami simulations, is 5 m (b).

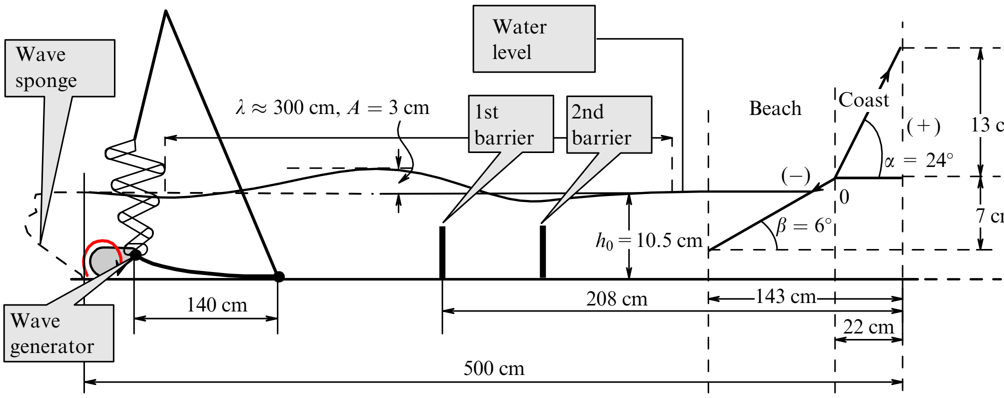

Figure 3. Schematic of the experimental setup.

which are 20 and 5 m in length. Figure 2a shows the longer channel and Fig. 2b shows the shorter one, which we used in our research. Our setup is schematically presented in Fig. 3. The left part displays a tsunami wave generator — a bent aluminum plate that is held pressed to the bottom by a catch, opposing the action of a stretched spring. When the catch releases the plate, it returns to its previous state driven by the spring and pushes some amount of water to the right, toward the 'beach' and the 'coast.' Centimeter grids are drawn on the beach and the coast, the positive one on the coast and the negative on the beach. They serve as gauges to measure the tsunami runup. The wavelength is 3 m, the wave amplitude is 3 cm, and the channel depth is 10.5 cm. The wavelength and amplitude of the tsunami are measured with wave height meters, each comprising two tantalum wires (Fig. 4) working as a capacitor with variable capacity, which is defined by the fluid height. Figure 5 plots the time dependence of tsunami elevation measured by one of the instruments. Figure 6 highlights the action of the wave generator: the catch holds the bent metallic plate (Fig. 6a, b), which then pushes water toward the shore (Fig. 6c).

The first barrier was placed at the distance 102 cm from the wave generator at the bottom of the channel, perpendicular to its axis, intercepting the channel up to a certain depth. A second, identical barrier was placed some distance further. The barriers were aluminum plates 3 mm thick and 50 cm wide (the channel width). We were interested in exploring how the height of the barriers and their separation affect the runup of water that reached the shore. With this aim, we varied both the height of the barriers and the distance between them during the experiments, while keeping the position of the first barrier fixed with respect to the wave generator (102 cm). The ratio of the barrier height to the depth was varied from 0.3 to 1.2.

Figure 4. Gauges used to measure the height.

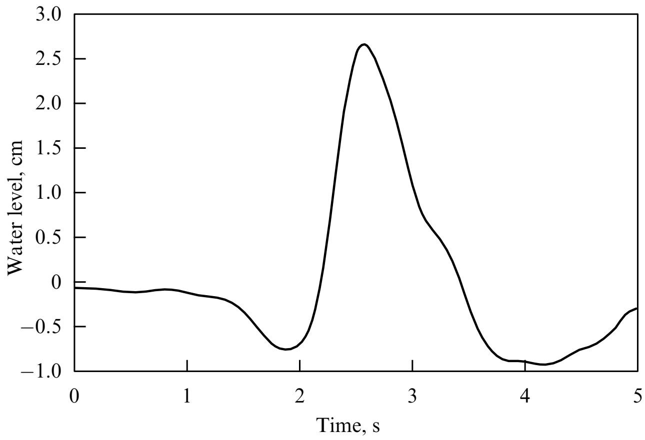

Figure 5. Time evolution of a tsunami as measured by one of the gauges.

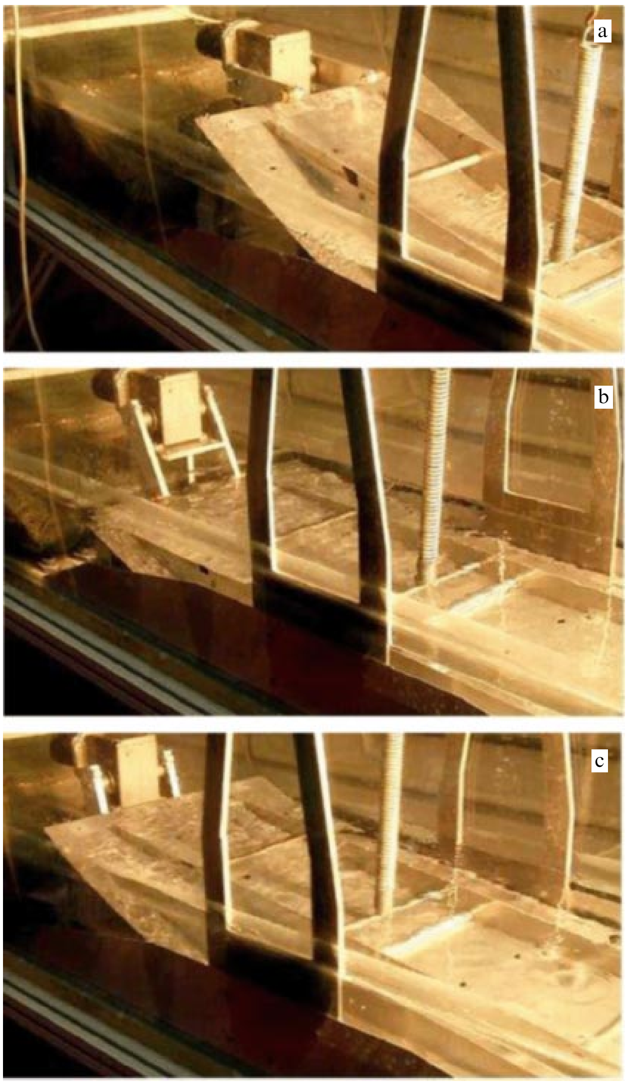

Figure 6. Frames showing the action of the trigger mechanism of the wave generator: (a) the catch that holds the plate is raised with the help of a motor above the plate; (b) the moment when the catch presses the plate down, the string is stretched; (c) the catch jumps off the plate edge, the string pulls the bend plate, and the entire volume of water above it is pushed to the right toward the coast.

A Fourier analysis of time evolution (Fig. 7) has shown that a mode with the period 3 s dominates the excited wave. Because the distance between the height gauges is known, the tsunami propagation speed is also known, and turns out to be 1 m s^{-1}. The prevalence of the three-second mode unambiguously determines the tsunami wavelength as 3 m. Because the wavelength λ greatly exceeds the fluid thickness h, the wave package can be regarded as a tsunami moving at the speed $c = \sqrt{gh}$.

Figure 8 shows the development of the runup across the beach and coast as the wave approaches the shore, from a gently sloping (Fig. 8a) and vertical front (Fig. 8b) to breaking and an S-wave (Fig. 8c) [24], and, finally, to wave dissipation on the coast. Here and below, we use a high-speed photo camera that allows taking up to 1200 frames per second (fps). In our experiments, we used a speed of 300 fps.

Figure 9 plots the dependence of tsunami runup on the height of a single barrier. Without the barrier, the runup is 10 cm. If the barrier height is close to the channel depth (10 cm), the runup is zero, i.e., water stays at the boundary between the beach and the coast. A barrier 12 cm in height, i.e., extending 1.5 cm over the water surface, reduces the runup height to −15 cm (beach).

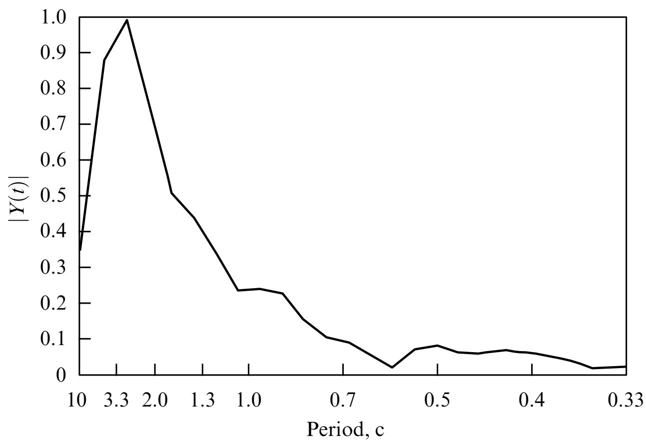

Figure 7. The Fourier spectrum of the wave package amplitude $|Y(t)|$ (see Fig. 5) produced by the wave generator.

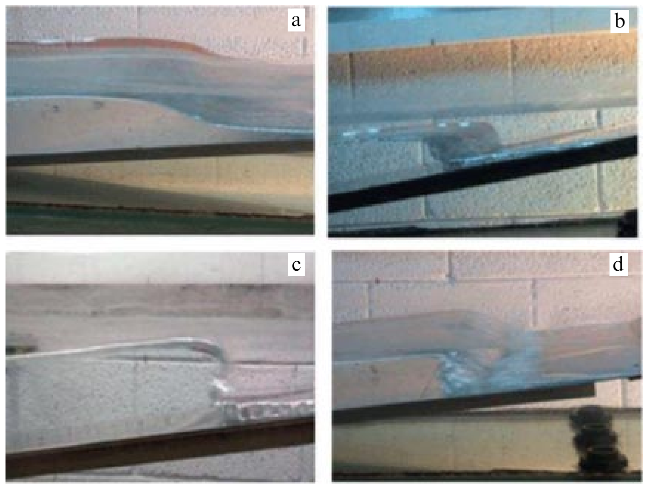

Figure 8. Photo frames showing the evolution of a wave package as it approaches the coast.

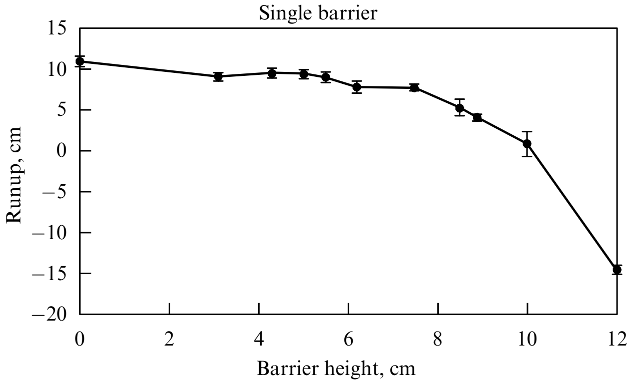

Figure 9. The runup as a function of the height of a single barrier.

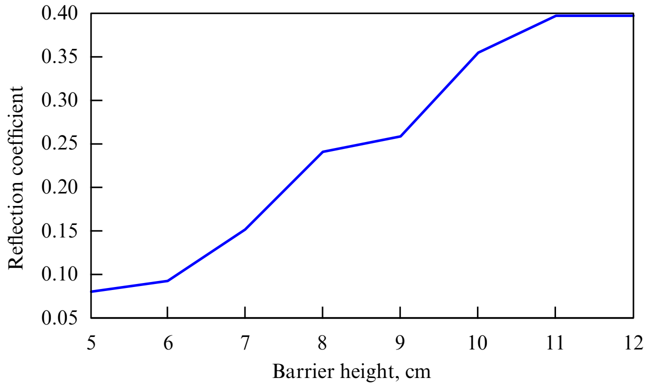

Figure 10. The tsunami reflection coefficient as a function of the barrier height. The depth of unperturbed fluid is 10.5 cm; therefore, barriers with the height 11 and 12 cm extend above the water surface.

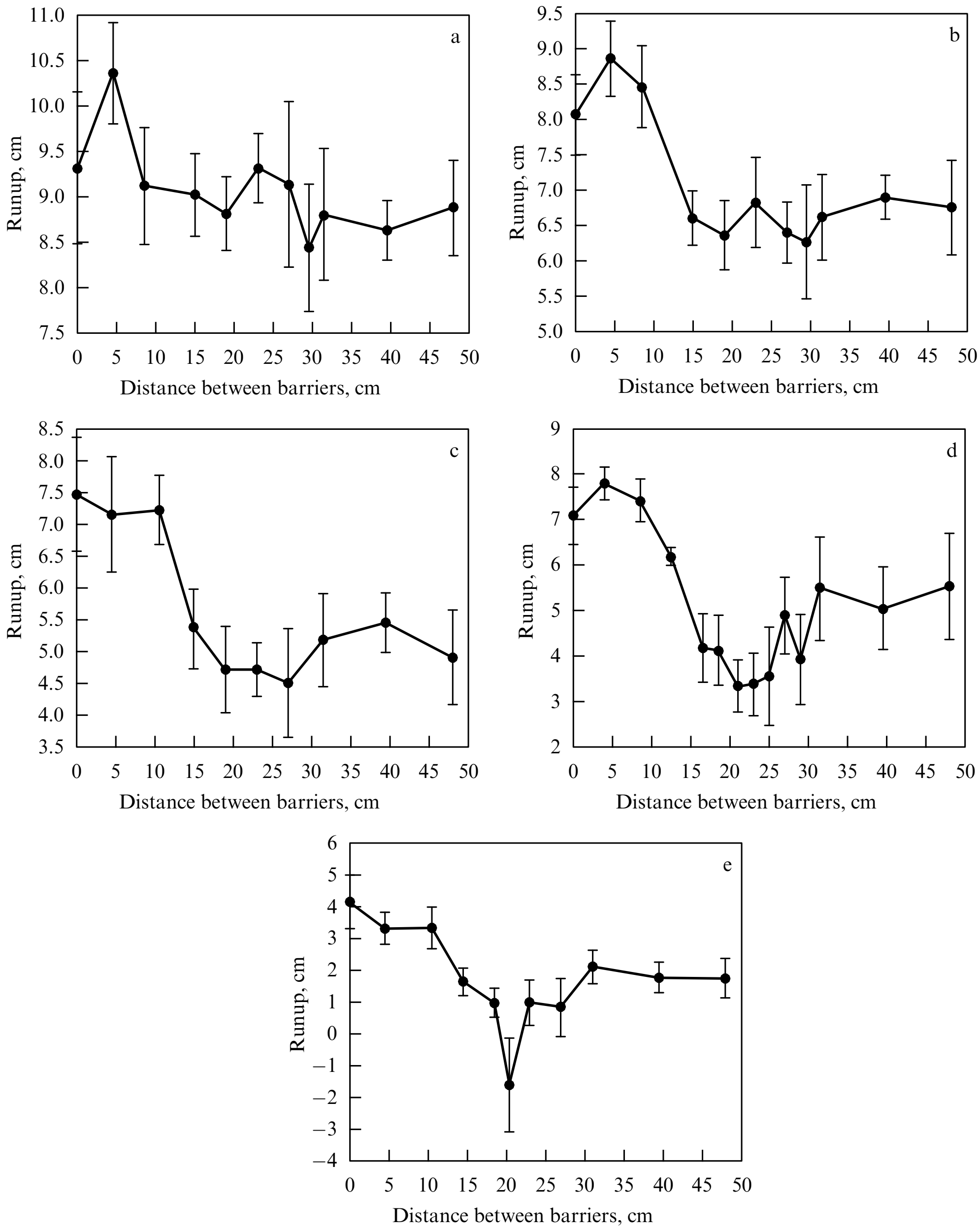

Figure 11. Plots showing the runup dependence on the distance between two bottom barriers of the same height. Height of barriers: 3.1 cm (a), 5.5 cm (b), 6.2 cm (c), 7.5 cm (d), and 8.5 cm (e).

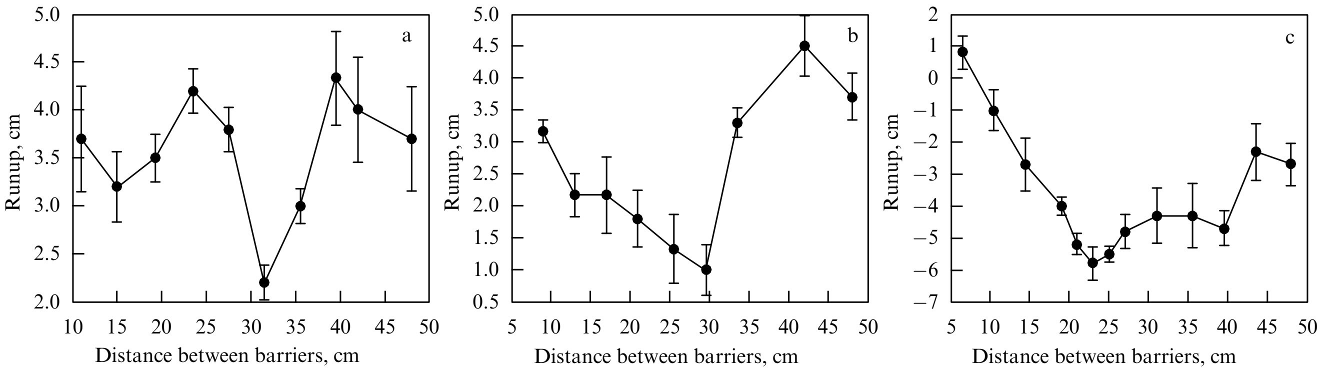

Figure 12. The same as in Fig. 11, but for a rough surface covering the beach and the coast. The height of double barriers is 3.0 cm (a), 5.5 cm (b), and 7.5 cm (c).

Figure 10 shows the dependence of the wave reflection coefficient on the height for a single barrier. Apparently, the maximum in the reflection coefficient (0.4) corresponds to the maximum barrier height (12 cm).

The wave runup was recorded by a high-speed photo camera. A wave excited in the channel is practically independent of the transverse coordinate and propagates along the channel as a bore wave. But as it approaches the coast, it starts to feel local defects in the tilted aluminum plate modeling the coastal zone, such as its surface roughness, micro cracks, or greasy spots, which eventually destroys the initially two-dimensional structure of the incident wave. The runup builds tongues or holes that disturb the frontal structure. Realizing this, we used the distance to the farthest wet point as a quantitative characteristics of runup.

The runup was estimated each time as the average over several (usually, 7–10) experimental realizations. The runup measured for the first run was always very different from that in subsequent experiments. The explanation is obvious: the properties of dry and wet surfaces are markedly different; in performing experiments, we therefore always discarded the results of the first one and used the rest (keeping the barrier height and distance between the barriers fixed) to compute the mean runup.

The dependence of runup on the distance between two similar barriers is presented in Fig. 11. The minimum in the runup occurring for a certain distance between the barriers was the more pronounced, the larger the barrier height. To gain more support for the existence of a minimum tsunami runup, we performed additional experiments in which the characteristics of the beach and coast were modified. In these experiments, they were covered with a hygroscopic paper. The wet surface becomes transparent and the underlying centimeter grid also allows accurate measurement of runup in this case. Such a thin hygroscopic layer not only effectively masks local inhomogeneities, roughness, or defects of the machine processing of a metallic surface, making the 'beach' surface smoother and more homogeneous, but also introduces additional friction affecting the runup. Figure 12 is similar to Fig. 11 and in the same manner shows the runup as a function of the distance between the barriers. But in the experimental series presented there, the properties of the beach and coast were modified by covering them with a rough hygroscopic paper. By comparing both figures, we can see that the minimum observed for the original, uncovered coast pronounced only for barriers exceeding 7.5 cm is well manifested for the rough coast even for small barriers.

The behavior of runup observed here, which is sensitive not only to underwater barriers but also to the distance between them, undoubtedly implies that the impact of a tsunami that reaches the coast can be controlled with such barriers. Bearing this in mind, in the last series of experiments, we explored the strength with which a tsunami hits an obstacle placed on the coast. Instead of near-bottom barriers fully intercepting the channel, we used small concrete tiles (7 cm in width and height and 0.8 cm thick). The tiles fell if two barriers 8 cm in height were installed at the bottom and the distance between them reached a maximum (48 cm). But the tiles held the strike and did not lose stability even for two shallower (7.5 cm) barriers when the distance between them was 25 cm, which corresponds to the minimum runup for such barriers (Fig. 12d).

The experiments conducted for various types of coast, despite quantitative differences, allow concluding that a considerable reduction in a tsunami hazard can be achieved with the help of single or double submerged barriers.

We now try to translate the results of our experiments to natural conditions. We estimate a characteristic size of bottom barriers and distances between them that would noticeably affect the runup of the wave on the shore. In the Appendix, we show that the laboratory model considered here allows a similarity transformation according to which the characteristic dimensions increase, e.g., by a factor n, while time changes by the factor $\sqrt{n}$. In our experiments, the water depth was 0.1 m. We assume that the wave approaches a coast 10 m deep, implying the scale factor $n = 10^2$. A wave with the length $\lambda = 3$ m and duration 3 s transforms into a wave 300 m in length and 30 s in duration. Because the length of oceanic waves seldom exceeds 100 m, a wave with the wavelength 300 m can be considered a short tsunami wave. The laboratory experiments have demonstrated that even small near-bottom obstacles crossing the tsunami path can noticeably suppress the wave on the coast if the separation between them is properly selected. For instance, barriers 3 m in height installed at the bottom of a 10 m layer 30 m apart can reduce the tsunami runup twofold (Fig. 12 a).

3. Conclusions

The experiments were conducted in a basin 5 m in length and 10.5 cm in depth. The wavelength of the generated wave was about 3 m, which allows referring to it as a tsunami. We used two types of barriers: single and double, with a variable distance between the barriers in the second case.

I. In experiments with single barriers,

1) we have confirmed the results of earlier experiments [15] that showed that a single barrier is capable of reducing the tsunami runup;

2) it was found that the runup is negligible only for unsubmerged barriers.

II. For the first time, experiments with double submerged barriers were conducted. They demonstrated that

1) double barriers are more efficient than single barriers of the same size in reducing the tsunami runup;

2) a minimum runup exists for a particular distance between two submerged barriers;

3) as the barrier height increases, the relative amplitude of the minimum runup decreases. The runup can be reduced virtually to zero for submerged barriers;

4) using the group-theory method of differential equations developed by Ovsyannikov [6], the parameters of experiments can be translated to natural conditions.

4. Appendix

The group of similarity transformations allowed by the Euler equations

Three-dimensional motion (including wave motion) of the ideal incompressible fluid in a layer $\eta(x, y, t) \geqslant z \geqslant h(x, y)$, where x and y are horizontal coordinates, in the presence of the force of gravity and in the absence of other external forces (bottom friction, the Coriolis force, etc.) and vorticity satisfy the Euler differential equations, which in vector notation take the form

$$\operatorname{div}\mathbf{v} = 0\,,$$
$$\frac{\partial \mathbf{v}}{\partial t} + (\mathbf{v}\nabla)\,\mathbf{v} = -\frac{1}{\rho}\frac{\partial p}{\partial \mathbf{r}} - \mathbf{g}\,,$$
$$\operatorname{rot}\mathbf{v} = 0\,,$$

or, in the component form,

$$\begin{aligned}
&\frac{\partial v_x}{\partial x} + \frac{\partial v_y}{\partial y} + \frac{\partial v_z}{\partial z} = 0\,,\\
&\frac{\partial v_x}{\partial t} + v_x\frac{\partial v_x}{\partial x} + v_y\frac{\partial v_x}{\partial y} + v_z\frac{\partial v_x}{\partial z} = -\frac{1}{\rho}\frac{\partial p}{\partial x}\,,\\
&\frac{\partial v_y}{\partial t} + v_x\frac{\partial v_y}{\partial x} + v_y\frac{\partial v_y}{\partial y} + v_z\frac{\partial v_y}{\partial z} = -\frac{1}{\rho}\frac{\partial p}{\partial y}\,,\\
&\frac{\partial v_z}{\partial t} + v_x\frac{\partial v_z}{\partial x} + v_y\frac{\partial v_z}{\partial y} + v_z\frac{\partial v_z}{\partial z} = -\frac{1}{\rho}\frac{\partial p}{\partial z} - g\,,\\
&\operatorname{rot}_x\mathbf{v} = \frac{\partial v_y}{\partial z} - \frac{\partial v_z}{\partial y} = 0\,, \quad \text{i.e.,} \quad \frac{\partial v_y}{\partial z} = \frac{\partial v_z}{\partial y}\,,\\
&\operatorname{rot}_y\mathbf{v} = \frac{\partial v_z}{\partial x} - \frac{\partial v_x}{\partial z} = 0\,, \quad \text{i.e.,} \quad \frac{\partial v_z}{\partial x} = \frac{\partial v_x}{\partial z}\,,\\
&\operatorname{rot}_z\mathbf{v} = \frac{\partial v_x}{\partial y} - \frac{\partial v_y}{\partial x} = 0\,, \quad \text{i.e.,} \quad \frac{\partial v_x}{\partial y} = \frac{\partial v_y}{\partial x}\,.
\end{aligned} \tag{1}$$

The following boundary conditions must be satisfied at the free surface and the bottom:

$$v_z = \frac{\mathrm{d}\eta(x,y,t)}{\mathrm{d}t} = \frac{\partial \eta}{\partial t} + \frac{\partial \eta}{\partial x}v_x + \frac{\partial \eta}{\partial y}v_y\,,\ p = 0 \text{ at } z = \eta\,, \tag{2}$$
$$\frac{\mathrm{d}z}{\mathrm{d}t} = \left(\frac{\partial z}{\partial t} = 0\right) + \frac{\partial z}{\partial x}v_x + \frac{\partial z}{\partial y}v_y = \frac{\partial z}{\partial x}v_x + \frac{\partial z}{\partial y}v_y\,,\ z = h\,.$$

The following notation is used in Eqs (1) and (2): v_x, v_y, and v_z are the velocity components along the x, y, and z axes, ρ is the density, p is the pressure, $\mathbf{g}$ is the gravity acceleration, η is the free surface elevation with respect to its unperturbed position, and h is the fluid depth.

We consider what happens if all linear dimensions are increased n-fold, i.e., when all dependent and independent variables are transformed as

$$x^* = nx\,,\ y^* = ny\,,\ z^* = nz\,,\ \eta^* = n\eta,\ h^* = nh\,. \tag{3}$$

We seek a similarity transform of the coordinates and variables for system of equations (1) and (2) that would preserve the equality between the right-hand and sides of the equations if the equations are satisfied for some solution (a set of parameters). To perform such an analysis, the system above can be conveniently rewritten in terms of displacements for the time interval ∂t in directions of the coordinate axes, ∂nx, ∂ny, and ∂nz. In particular, the component v_x of the full velocity $\mathbf{v}$ along the x axis can be written as

$$v_x = \frac{\partial nx}{\partial t}\,.$$

After the corresponding substitutions, Eqs (1) and 2 take the form

$$\frac{\partial^2 nx}{\partial x\,\partial t} + \frac{\partial^2 ny}{\partial y\,\partial t} + \frac{\partial^2 nz}{\partial z\,\partial t} = 0\,, \tag{4}$$
$$\frac{\partial^2 nx}{\partial t\,\partial t} + \frac{\partial nx}{\partial t}\frac{\partial^2 nx}{\partial x\,\partial t} + \frac{\partial ny}{\partial t}\frac{\partial^2 nx}{\partial y\,\partial t} + \frac{\partial nz}{\partial t}\frac{\partial^2 nx}{\partial z\,\partial t} = -\frac{1}{\rho}\frac{\partial p}{\partial x}\,, \tag{5}$$
$$\frac{\partial^2 ny}{\partial t\,\partial t} + \frac{\partial nx}{\partial t}\frac{\partial^2 ny}{\partial x\,\partial t} + \frac{\partial ny}{\partial t}\frac{\partial^2 ny}{\partial y\,\partial t} + \frac{\partial nz}{\partial t}\frac{\partial^2 ny}{\partial z\,\partial t} = -\frac{1}{\rho}\frac{\partial p}{\partial y}\,, \tag{6}$$
$$\frac{\partial^2 nz}{\partial t\,\partial t} + \frac{\partial nx}{\partial t}\frac{\partial^2 nz}{\partial x\,\partial t} + \frac{\partial ny}{\partial t}\frac{\partial^2 nz}{\partial y\,\partial t} + \frac{\partial nz}{\partial t}\frac{\partial^2 nz}{\partial z\,\partial t} = -\frac{1}{\rho}\frac{\partial p}{\partial z} - g\,, \tag{7}$$
$$\frac{\partial^2 nz}{\partial t\,\partial y} = \frac{\partial^2 ny}{\partial t\,\partial z}\,,\ \frac{\partial^2 nx}{\partial t\,\partial z} = \frac{\partial^2 nz}{\partial t\,\partial x}\,,\ \frac{\partial^2 ny}{\partial t\,\partial x} = \frac{\partial^2 nx}{\partial t\,\partial y}\,. \tag{8}$$

For small flow velocities, the pressure in the body of water differs from the hydrostatic pressure only slightly:

$$p = \rho g\big(\eta(x, y, t) - z\big)\,.$$

After this substitution, the right-hand side of Eqn (7) vanishes, while the right-hand side of Eqn (5) and Eqn (6) contain the quantities

$$g\,\frac{\partial n\eta}{\partial x} \quad \text{and} \quad g\,\frac{\partial n\eta}{\partial y}\,. \tag{9}$$

It is easy to see that with the new variables substituted, all terms increase n-fold if t is unchanged. To preserve the equality of both sides of the equations, t should also be transformed by the factor $\sqrt{n}$. Hence, the change of variables in (3) and the time transformation

$$t^* = \sqrt{n}t \tag{10}$$

is an admissible similarity transformation group [24] for Euler equations (1) and (2). In other words, if a solution of the problem in Eqns (1) and (2) is found, then the same solution transformed in agreement with Eqns (3) and (10) solves the equation in the case where all linear sizes are increased n-fold and time is stretched by the factor $\sqrt{n}$.

References

1. Solov'ev S L et al. *Tsunami v Sredizemnom More, 2000 g. do n.e. — 1991 g.* (Tsunami in the Mediterranean, 2000 BC) (Moscow: Nauchnyi Mir, 1997)
2. Stephenson F et al. "Catalogue of tsunamis. British Columbia, Canada: 1700 – 2007", Preprint (Moscow: Yanus-K., 2007)
3. Levin B V, Nosov M A *Fizika Tsunami i Rodstvennykh Yavlenii v Okeane* (Physics of Tsunamis and Related Phenomena in the Ocean) (Moscow: Yanus-K, 2005)
4. Gutenberg B "Tsunamis and earthquakes" *Bull. Seismolog. Soc. Am.* **29** 517 (1939)
5. Pelinovskii E N *Nelineinaya Dinamika Voln Tsunami* (Nonlinear Dynamics of Tsunami Waves) (Gorkii: IPF AN SSSR, 1982)
6. Pelinovskii E N *Gidrodinamika Voln Tsunami* (Hydrodymamics of Tsunami Waves) (Nizhny Novgorod: IPF RAN, 1996)
7. Kurkin A A, Pelinovskii E N, Slyunyaev A V, in *Nelineinye Volny 2004* (Nonlinear Waves 2004) (Ed. A V Gaponov-Grekhov) (Nizhny Novgorod: IPF RAN, 2005)
8. Ma Q (Ed.) *Advances in Numerical Simulation of Nonlinear Water Waves* (Advances in Coastal and Ocean Engineering, Vol. 11) (Singapore: World Scientific, 2010)
9. Pelinovskii E N *Vulkanolog. Seismolog.* (5) 79 (1988)
10. Marchuk An G, Chubarov L B, Shokin Yu I *Chislennoe Modelirovanie Voln Tsunami* (Numerical Simulation of Tsunami Waves) (Novosibirsk: Nauka, 1983)
11. Shokin Yu I et al. *Vychislitel'nyi Eksperiment v Probleme Tsunami* (Computational Experiment in the Tsunami Problem) (Exec. Ed. V M Fomin) (Novosibirsk: Nauka, 1989)
12. Berry M V *Proc. R. Soc. Lond. A* **463** 3055 (2007)
13. Landau L D, Lifshitz E M *Gidrodinamika* (Fluid Mechanics) (Moscow: Nauka, 1986) [Translated into English (Oxford: Pergamon Press, 1987)]
14. International Maritime Organization, Maritime knowledge centre. Information resource "On Tsunami Disaster in South Asia", Information Sheet No. 4, May, 2009
15. Wiegel R *J. Waterways Harbors Div., ASCE* **86** 1 (1960)
16. Liu R L-F, Abbaspour M *J. Waterway, Port, Coastal Ocean Div., ASCE* **108** 479 (1982)
17. Blackmore P A, Hewson P J *Coastal Eng.* **8** 331 (1984)
18. Chan E S, Melville W K *Proc. R. Soc. Lond. A* **417** 95 (1988)
19. Ramsden J D "Tsunamis: Forces on a vertical wall caused by long waves, bores, and surges on a dry bed", Technical Report No. KH-R-54 (Pasadena, Calif.: California Institute of Technology, 1993)
20. Goda Y *Adv. Ocean Eng.* **15** 464 (2000)
21. Gao Xueping *J. Hydrodyn. B* **1** 28 (2001)
22. Sorensen R M *Basic Coastal Engineering* 3rd ed. (New York: Springer Sci., 2006)
23. Lighthill J *Waves in Fluids* (Cambridge: Cambridge Univ. Press, 1978) [Translated into Russian (Moscow: Mir, 1981)]
24. Ovsyannikov L V *Gruppovye Svoistva Differentsial'nykh Uravnenii* (Group Properties of Differencial Equations) (Novosibirsk: Izd. SO AN SSR, 1962)